Long-range potential fluctuations and $1/f$ noise in hydrogenated amorphous silicon

B. V. Fine[1,3*], J. P. R. Bakker[2], and J. I. Dijkhuis[2]
[1]*Spinoza Institute and* [2]*Debye Institute, Utrecht University, P.O. Box 80000, 3508 TA Utrecht, Netherlands*
[3]*Max Plank Institute for the Physics of Complex Systems, Noethnitzer Str. 38, D-01187, Dresden, Germany*
(Dated: June 4, 2003)

We present a microscopic theory of the low-frequency voltage noise (known as "$1/f$" noise) in μm-thick films of hydrogenated amorphous silicon. This theory traces the noise back to the long-range fluctuations of the Coulomb potential created by deep defects, thereby predicting the *absolute* noise intensity as a function of the distribution of defect activation energies. The predictions of this theory are in very good agreement with our own experiments in terms of both the absolute intensity and the temperature dependence of the noise spectra.

PACS numbers: 71.55.Jv, 72.70.+m, 73.50.Td, 73.61.Jc

I. INTRODUCTION

When electric current flows through a resistor, strong low-frequency voltage noise superposed on the thermal Johnson-Nyquist noise[1,2] is generally observed. The spectrum of that excess noise has shape close to $1/f$, where f is frequency[3]. In recent decades, the model, according to which the $1/f$ noise is produced by an ensemble of two-state systems having broadly distributed activation energies (BDAE)[4,5,6], has enjoyed a lot of success. However, the BDAE model addresses neither the origin of the two-state systems nor the noise mechanism, thus leaving the absolute noise intensity as an adjustable parameter. The lack of direct microscopic calculations predicting the absolute noise intensity, while being a glaring theoretical gap as such, also fuels an old but still continuing debate over the question of what actually fluctuates — the number of carriers or their mobility[3].

In this work, we present a theoretical and experimental investigation of $1/f$ noise in hydrogenated amorphous silicon (a-Si:H). Our theory links the noise to the fluctuations of the number of carriers, predicts the absolute noise intensity, and also allows us to extract novel and useful information about the defects in this important material[16].

This theory can be outlined as follows: Hydrogenated amorphous silicon has a significant number of deep defects known as dangling bonds. Thermal fluctuations of the numbers of electrons occupying the dangling bonds cause long-range potential fluctuations, which give rise to fluctuations of the local densities of carriers, which, in turn, lead to resistance fluctuations, which, in the presence of current, manifest themselves as voltage noise. It is the inclusion of the long-range potential fluctuations into the above scheme that distinguishes our treatment from many similar theoretical proposals.

II. EXPERIMENTAL SETUP

The $1/f$ noise in a-Si:H has been studied in the literature in a variety of experimental settings (see e.g. Refs.[7,8,9,10,11,12,13,14,15]), and exhibited certain features, which depend on numerous details of each particular experiment. In this work we present a fully developed quantitative study of only one situation, which corresponds to our own experiments. Other experimental settings will only be discussed briefly in the end of the paper.

The present study is focused on an $n-i-n$ film of a-Si:H, where n stands for a 40nm-thick electron doped layer, and i for an undoped layer of thickness $d = 0.91\mu$m. The $n-i-n$ structure is grown by plasma enhanced chemical vapor deposition (PECVD) on a highly conductive wafer of crystaline silicon. The contact layer on the top of the structure consists of a 30nm-thick film of titanium followed by 30nm-thick film of copper. The film has area $A = 0.56\text{cm}^2$. It is thermally annealed and then protected from light. We observe and analyse the voltage noise spectra at frequencies $f = 1 \div 10^4$ Hz and temperatures $T = 340 \div 434$ K in the presence of electric current flowing perpendicular to the plane of the film. Other details of our experimental setup are described in Ref.[10].

III. FORMULATION OF THE THEORETICAL PROBLEM

Now we turn to the theoretical derivation of the noise spectrum under the above experimental conditions. The central and, presumably, quite general part of this derivation is Section IV. Most of the rest is specific to a-Si:H and to the experimental setting considered.

Our goal is to compute voltage noise spectrum $S_V(f)$ expressed as:

$$\frac{S_V(f)}{V^2} = 4\int_0^\infty C_V(t)\cos(2\pi f t)\ dt, \tag{1}$$

where V is the applied voltage, and

$$C_V(t) = \frac{\langle \delta R(t)\delta R(0)\rangle}{R_0^2}. \tag{2}$$

Here, R_0 is the average resistance of the film, and $\delta R(t)$ is the equilibrium resistance noise. As usual[3], the link between the resistance noise and the voltage noise is established experimentally by observing that $S_V(f) \propto V^2$.

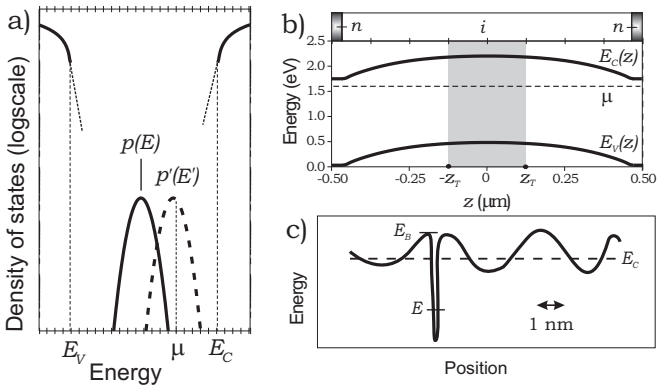

FIG. 1: (a) Sketch of the density of states in the center of the undoped layer. (b) Band bending profile. The gray stripe represents the "uniform resistivity layer" defined in the text. (c) Cartoon of a deep defect surrounded by medium-range structural disorder. Note: $e\phi(t,\mathbf{r})$ fluctuates on a much longer lengthscale and with much smaller amplitude.

The density of states of undoped a-Si:H is shown in Fig. 1a. It is characterized by a band gap of 1.8 eV between the mobility edges E_v and E_c in the valence and conduction bands, respectively. The proximity of the n-layers induces band bending in the undoped layer as shown in Fig 1b. Around the center of the film $E_c(z) = E_{c0} - \beta z^2$, where the z-axis is directed perpendicular to the film, $E_{c0} = \mu + 0.63\,\mathrm{eV}$, μ is the chemical potential, and $\beta = 1.6\,\mathrm{eV}/\mu\mathrm{m}^2$. The difference $E_{c0} - \mu$ was obtained experimentally as the conductivity activation energy, while the value of β was found numerically (cf.[17]).

Since μ is significantly closer to E_c than to E_v, the resistivity ρ is inversely proportional to the density of conduction electrons n_e. Keeping in mind that $n_e \propto \exp\left(-\frac{E_c-\mu}{k_BT}\right)$, we obtain $\rho(z) = X\exp\left(\frac{E_c(z)-\mu}{k_BT}\right)$, which is strongly peaked around $z = 0$. Here X is a proportionality coefficient, and k_B is the Boltzmann constant. The total film resistance can then be found as $R_0 = \frac{1}{A}\int \rho(z)dz \approx \frac{\rho(0)}{A}\sqrt{\frac{\pi k_BT}{\beta}}$.

To simplify the treatment we replace the actual profile of $\rho(z)$ by a layer of constant resistivity $\rho_0 = \rho(0)$ spreading along the z-axis between $-z_T$ and z_T (see Fig. 1b). We require the resistance of this constant resistivity layer to be equal to R_0, which gives

$$z_T = \frac{1}{2}\sqrt{\frac{\pi k_BT}{\beta}} \tag{3}$$

(typical value: 0.13μm).

IV. CORRELATION FUNCTION

The resistivity within the "constant resistivity layer" still fluctuates as a consequence of the fluctuations of the screened Coulomb potential $\phi(t,\mathbf{r})$ created by deep defects:

$$\phi(t,\mathbf{r}) = \sum_i \frac{\Delta q_i(t)}{\epsilon|\mathbf{r}-\mathbf{a}_i|}\exp\left(-\frac{|\mathbf{r}-\mathbf{a}_i|}{r_{s_i}}\right). \tag{4}$$

Here $\Delta q_i(t)$ is the fluctuation of the ith defect charge with respect to its average value, $\mathbf{a}_i$ the position the defect, r_{s_i} the screening radius of that defect, and $\epsilon = 12$ the dielectric constant. The defects causing the potential fluctuations may be located outside of the constant resistivity layer. [Note: the above formula does not include large static component of the random Coulomb potential.]

When the local potential $\phi(t,\mathbf{r})$ fluctuates, the mobility edge tracks it, i.e. $E_c(t,\mathbf{r}) = E_{c0} + e\phi(t,\mathbf{r})$, where e is the electron charge. Since μ does not shift with $e\phi(t,\mathbf{r})$, the density of conduction electrons re-equilibrates following $E_c(t,\mathbf{r})$ on the timescale of electron drift from the uniform resistivity layer to the n-layers (and then to the contact layers). Because of the strong band bending, the drift takes less than 10^{-7}s, i.e. the re-equilibration is effectively instantaneous on the timescales of the noise studied ($\frac{2\pi}{f} \sim 10^{-4} \div 1$ s). The resistivity can thus be rewritten as $\rho(t,\mathbf{r}) = X\exp\left(\frac{E_c(t,\mathbf{r})-\mu}{k_BT}\right)$. Assuming for a moment [and proving later] that $|e\phi(t,\mathbf{r})| \ll k_BT$, we expand $\rho(t,\mathbf{r}) = \rho_0 + \delta\rho(t,\mathbf{r})$, where $\rho_0 = X\exp\left(\frac{E_{c0}-\mu}{k_BT}\right)$, and

$$\delta\rho(t,\mathbf{r}) = \frac{e\phi(t,\mathbf{r})}{k_BT}\rho_0. \tag{5}$$

For $\delta\rho \ll \rho_0$, the fluctuation of the total resistance is

$$\delta R(t) = \frac{1}{A^2}\int_{\mathcal{V}} \delta\rho(t,\mathbf{r})d^3r, \tag{6}$$

where $\mathcal{V}$ is the space inside the constant resistivity layer. Substituting $R_0 = \frac{2z_T\rho_0}{A}$ and $\delta R(t)$ given by Eq.(6) into Eq.(2) and then using Eq.(5), we obtain

$$C_V(t) = \left(\frac{e}{2k_BTz_TA}\right)^2 \int_{\mathcal{V}} d^3\mathbf{r}\int_{\mathcal{V}} d^3\mathbf{r}'\langle\phi(t,\mathbf{r})\phi(0,\mathbf{r}')\rangle. \tag{7}$$

V. DESCRIPTION OF DEFECTS

In order to evaluate $\langle\phi(t,\mathbf{r})\phi(0,\mathbf{r}')\rangle$, we have to describe the deep defects in the undoped layer of a-Si:H[18].

There exist both theoretical arguments and experimental evidence[19] indicating that the concentration of defects in the undoped layer should be greater in the vicinity of the n-layers and then decay towards the center on the lengthscale of about 0.5μm. Here, however, in order to simplify the theoretical treatment, we assume that the defect concentration across the entire undoped layer has a constant value, which we estimate as[18] $n_D = 6\times10^{15}\,\mathrm{cm}^{-3}$.

Each defect has 4 possible states: one zero-electron state D^+, two one-electron states D^0, and one two-electron state, D^-. We assume a Gaussian probability distribution

$$p(E) = \frac{1}{\sqrt{2\pi}\Delta E}\ e^{-\frac{(E-E_0)^2}{2\Delta E^2}} \tag{8}$$

for energy E of an electron occupying the D^0 state. Here $E_0 = \mu - 0.22\,\mathrm{eV}$ and $\Delta E = 0.15\,\mathrm{eV}$. Energy E, as such, is associated only with the $D^+ \leftrightarrow D^0$ transition. The $D^0 \leftrightarrow D^-$ transition, which requires capturing the second electron by the same defect, is characterized by energy $E' = E + U$, where $U = 0.2\,\mathrm{eV}$ is the correlation energy. Therefore, the corresponding probability distribution is

$$p'(E') = \frac{1}{\sqrt{2\pi}\Delta E} e^{-\frac{(E'-E_0-U)^2}{2\Delta E^2}}. \tag{9}$$

We shall treat the $D^+ \leftrightarrow D^0$ transitions independently from the $D^0 \leftrightarrow D^-$ transitions, which is justified as long as $\exp\left(-\frac{U}{k_BT}\right) \ll 1$.

The noise spectrum obtained later will depend only weakly on defect parameters n_D, E_0, U and ΔE, mainly through a weak dependence on one combination of them — the density of defect states at the chemical potential. That combination, in turn, is not very sensitive to the choice of E_0 and U.

Using the equilibrium description[20] of the D^+, D^0 and D^- states, we obtain the mean squared charge fluctuations for the $D^+ \leftrightarrow D^0$ transition:

$$\langle \Delta q^2(E) \rangle_+ = \frac{1}{4}\, e^2\, \mathrm{sech}^2\left(\frac{E-\mu}{2k_BT} - c\right); \tag{10}$$

where $c = \frac{1}{2}\ln 2$. For the $D^0 \leftrightarrow D^-$ transition:

$$\langle \Delta q^2(E') \rangle_- = \frac{1}{4}\, e^2\, \mathrm{sech}^2\left(\frac{E'-\mu}{2k_BT} + c\right). \tag{11}$$

In order to escape from a deep defect, an electron should reach the mobility edge E_c. However, the activation barriers E_B (indicated in Fig.1c) can vary as a result of the *medium-range* disorder of the amorphous structure (on a lengthscale of $1 \div 10\,\mathrm{nm}$). We assume a Gaussian probability distribution for the values of E_B:

$$P(E_B) = \frac{1}{\sqrt{2\pi}\Delta E_B} \exp\left(-\frac{(E_B - E_{B0})^2}{2\Delta E_B^2}\right). \tag{12}$$

where E_{B0} and ΔE_B are to be extracted from the experimental spectra. These are the only two adjustable parameters in our treatment. They will affect the spectral shape, but not the integrated noise intensity.

The fluctuation rate for the $D^+ \leftrightarrow D^0$ transition is[21]

$$\frac{1}{\tau_+(E, E_B)} = \omega_0(E_B)\left[e^{-\frac{E_B-\mu}{k_BT}} + \frac{1}{2}\, e^{-\frac{E_B-E}{k_BT}}\right]; \tag{13}$$

and for the $D^0 \leftrightarrow D^-$ transition:

$$\frac{1}{\tau_-(E', E_B)} = \omega_0(E_B)\left[\frac{1}{2}\, e^{-\frac{E_B-\mu}{k_BT}} + e^{-\frac{E_B-E'}{k_BT}}\right], \tag{14}$$

where the attempt frequency is estimated from the detailed balance condition as

$$\omega_0(E_B) = v_{th}\ \sigma\ \mathcal{N}_c(E_B) \tag{15}$$

Here, $v_{th} = \sqrt{3k_BT/m_e^*}$ is the thermal velocity of conduction electrons; m_e^* their effective mass ($m_e^* \approx 0.4 m_e = 3.64 \cdot 10^{-28}\mathrm{g}$); $\sigma = 10^{-15}\,\mathrm{cm}^2$ the cross-section of electron capture by D^+ or D^0 defect; and $\mathcal{N}_c(E_B) \approx N_c(E_B)\, k_BT$ the "concentration" of thermally accessible electronic states with energies above E_B; $N_c(E_B) = N_c(E_{c0})\sqrt{(E_B - E_{c0} + \varepsilon_c)/\varepsilon_c}$ the empirical fit to the density of states above the mobility edge; $N_c(E_{c0}) = 4 \times 10^{21}\,\mathrm{eV}^{-1}\mathrm{cm}^{-3}$; and $\varepsilon_c = 0.02\,\mathrm{eV}$. The typical value of $\omega_0(E_B)$ is then $10^{13}\,\mathrm{s}^{-1}$.

Next we evaluate the screening radius. Since the screening by the conduction electrons in the undoped layer can be neglected in view of their very small concentration ($10^{10} \div 10^{13}\mathrm{cm}^{-3}$), two other screening mechanisms should be considered, namely: (i) by the n-layers together with the contact layers; and (ii) by the defects in the undoped layer.

We describe the first mechanism as a perfect screening by metallic surfaces. In other words, we assume that a defect in the undoped layer is screened by the infinite set of its mirror images constructed with respect to the mirror planes located at $z = \pm d/2$. Although the screening law due to this mechanism is not exponential, we obtain the best possible value for r_s entering Eq.(4) as the distance from the defect to the point, where the screened potential is factor of $e = 2.718...$ smaller than the bare Coulomb potential. We have found numerically that r_s has angular dependence, which is such that, for a defect located at $z = 0$, $r_{sx} = r_{sy} = 0.54d$, and $r_{sz} = 0.38d$. We then approximate the screening radius due to this mechanism as

$$r_{s1} = (r_{sx} r_{sy} r_{sz})^{1/3} = 0.48d. \tag{16}$$

The second screening mechanism is similar to that of Thomas-Fermi. It can be described as follows: When the potential fluctuates due to charge fluctuation on a given defect, the energies E and E' of the neighboring defects become shifted. In response, those neighboring defects change their occupation numbers thus screening the potential of the defect, which originally caused the fluctuation. The equilibrium description of this mechanism[22] results in the screening radius

$$r_{\mathrm{eq}} = \sqrt{\frac{\epsilon}{4\pi e^2\ n_D \nu(T)}}, \tag{17}$$

where

$$\nu(T) = \frac{1}{4k_BT}\left\{\int_{-\infty}^{\infty} \tilde{p}(E)dE + \int_{-\infty}^{\infty} \tilde{p}'(E')dE'\right\}; \tag{18}$$

$$\tilde{p}(E) = p(E)\,\mathrm{sech}^2\left(\frac{E-\mu}{2k_BT} - c\right), \qquad (19)$$

and

$$\tilde{p}'(E') = p'(E')\,\mathrm{sech}^2\left(\frac{E'-\mu}{2k_BT} + c\right). \qquad (20)$$

The value of $\nu(T)$ depends on T very weakly. The product $n_D\nu(0)$ should be recognized as the density of the defect states at the chemical potential.

The equilibrium description of screening is applicable, when the sources of the Coulomb potential are static, and thus all the defects can contribute to screening. However, if a given defect fluctuates on time scale τ, its potential can only be screened by other defects fluctuating on timescales not slower than τ. To take this observation into account, we simply multiply n_D in formula (17) by $b(\tau)$, the fraction of defects that fluctuate fast enough to take part in the screening of a defect characterized by the fluctuation time τ. We estimate that fraction as

$$b(\tau) = \frac{1}{4k_BT\nu(T)}\left\{\int_{\mathcal{E}_+(\tau)} \tilde{p}(E)\,P(E_B)\,dE\,dE_B + \int_{\mathcal{E}_-(\tau)} \tilde{p}'(E')\,P(E_B)\,dE'\,dE_B\right\}, \qquad (21)$$

where $\mathcal{E}_+(\tau)$ is the integration region limited by condition $\tau_+(E,E_B) < \tau$, and $\mathcal{E}_-(\tau)$ the integration region limited by $\tau_-(E',E_B) < \tau$. The screening radius due to the second mechanism thus becomes

$$r_{s2}(\tau) = \sqrt{\frac{\epsilon}{4\pi e^2 n_D \nu(T) b(\tau)}}. \qquad (22)$$

For the slower fraction of defects, $r_{s2}(\tau)$ approaches $r_{\mathrm{eq}} \approx 0.18\,\mu$m, which is shorter than $r_{s1} = 0.43\,\mu$m. At the same time, for the faster ones, r_{s2} is very large, i.e. they are predominantly screened by the first mechanism. We, therefore, approximate the combined effect of the two mechanisms by using the following expression for the screening radius:

$$r_s^{-1}(\tau) = r_{s1}^{-1} + r_{s2}^{-1}(\tau). \qquad (23)$$

The typical value of r_s given by Eq.(23) is $r_s^* = 0.2\,\mu$m.

VI. EVALUATION OF THE NOISE SPECTRUM

Now we are in position to evaluate $\langle\phi(t,\mathbf{r})\phi(0,\mathbf{r}')\rangle$ with $\phi(t,\mathbf{r})$ given by Eq.(4).

Since an electron emitted by one deep defect is most likely absorbed not by another defect but by the contact layer, it is appropriate to assume that different defects fluctuate independently, which implies that, for $i \neq j$, $\langle\Delta q_i(t)\Delta q_j(0)\rangle = 0$. Keeping also in mind that

$$\langle\Delta q_i(t)\Delta q_i(0)\rangle = \langle\Delta q_i^2\rangle \exp(-t/\tau_i), \qquad (24)$$

we take the disorder average of $\phi(t,\mathbf{r})\phi(0,\mathbf{r}')$, i.e. we replace the discrete summation by the integrations over the relevant probability distributions. This gives

$$\langle\phi(t,\mathbf{r})\phi(0,\mathbf{r}')\rangle = \frac{n_D}{\epsilon^2}\int dE_B P(E_B)\ \left\{\int dE\,p(E)\,F(\mathbf{r},\mathbf{r}',\tau_+(E,E_B))\,\langle\Delta q(E)^2\rangle_+\,\exp\left(-\tfrac{t}{\tau_+(E,E_B)}\right) + \int dE' p'(E')\,F(\mathbf{r},\mathbf{r}',\tau_-(E',E_B))\,\langle\Delta q(E')^2\rangle_-\,\exp\left(-\tfrac{t}{\tau_-(E',E_B)}\right)\right\}, \qquad (25)$$

where

$$F(\mathbf{r},\mathbf{r}',\tau) \equiv \int \frac{\exp\left(-\frac{|\mathbf{r}-\mathbf{a}|+|\mathbf{r}'-\mathbf{a}|}{r_s(\tau)}\right)}{|\mathbf{r}-\mathbf{a}|\ |\mathbf{r}'-\mathbf{a}|}d^3\mathbf{a} \approx 2\pi r_s(\tau)\exp\left(-\frac{|\mathbf{r}-\mathbf{r}'|}{r_s(\tau)}\right). \qquad (26)$$

The approximation in Eq.(26) can be justified by observing that the main spatial dependence of the integral for $F(\mathbf{r},\mathbf{r}',\tau)$ has form $\exp\left(-\frac{|\mathbf{r}-\mathbf{r}'|}{r_s(\tau)}\right)$, and then the natural choice for the prefactor is $F(0,0,\tau) = 2\pi r_s(\tau)$ (obtained by direct integration).

From Eq.(25), the value of $|e\phi(t,\mathbf{r})|$ can be estimated as: $e\sqrt{\langle\phi^2(0,0)\rangle} \approx e^2\epsilon^{-1}\sqrt{2\pi n_D\nu(T)k_BTr_s^*} \sim 3.5$meV. Since $k_BT \sim 30$meV, the assumption $|e\phi(t,\mathbf{r})| \ll k_BT$ made earlier was adequate.

Finally, we evaluate $C_V(t)$ by substituting Eq.(25) into Eq.(7), and then take the Fourier transform (1) to obtain

$$\frac{S_V(f)}{V^2} = \frac{2\pi^2e^4n_D}{\epsilon^2(k_BT)^2Az_T^2} \times \int dE_B P(E_B)\left\{\int D(f,\tau_+(E,E_B))\tilde{p}(E)dE + \int D(f,\tau_-(E',E_B))\tilde{p}'(E')dE'\right\}, \qquad (27)$$

where

$$D(f,\tau)=\frac{\tau r_s^4(\tau)\Big[4z_T-3r_s(\tau)+e^{-\frac{2z_T}{r_s(\tau)}}(2z_T+3r_s(\tau))\Big]}{1+4\pi^2f^2\tau^2}. \tag{28}$$

Recalling the approximations associated with (i) the assumption of the constant resistivity layer; (ii) the assumption of the constant profile of defect concentration; (iii) the treatment of the screening radius; and (iv) the evaluation of $F(\mathbf{r},\mathbf{r}',\tau)$ (Eq.(26)), we estimate that the integrated noise intensity obtained from Eq.(27) entails a factor of two theoretical uncertainty for the noise mechanism considered.

The complex appearance of Eq.(27) is due to the fact that it includes separate terms for the two transitions $D^+ \leftrightarrow D^0$ and $D^0 \leftrightarrow D^-$. Such a separation is necessary only because the expressions (13, 14) for the activation times τ_+ and τ_- are slightly different from each other. This difference, however, vanishes if one assumes that the width of the distributions $\tilde{p}(E)$ and $\tilde{p}'(E')$ is much smaller than the width of $P(E_B)$, i.e. $2k_BT \ll \Delta E_B$.

The complicated form of the numerator in the right-hand side of Eq.(28) is the analytic result of the two integrations (7) over the volume of the "constant resistivity" layer. This expression reflects the competition between two length scales: the half-thickness of that layer (z_T) and the screening radius (r_s). In the "thin layer limit" $z_T \ll r_s$, the expression in the square brackets in Eq.(28) can be approximated by $\frac{2z_T^2}{r_s}$, whereas in the "bulk limit" $z_T \gg r_s$ that expression approaches $4z_T$.

Now we simplify Eq.(27) by taking limits $z_T \ll r_s$, $2k_BT \ll \Delta E_B$ and substituting $\nu(T)=\frac{1}{2\Delta E}$ (just an approximate numerical fact), which gives

$$\frac{S_V(f)}{V^2}=\frac{8\pi^2e^4n_D}{\epsilon^2k_BT\Delta EA}\int\frac{\tau_0(E_B)r_s^3\left(\tau_0(E_B)\right)P(E_B)dE_B}{1+4\pi^2f^2\tau_0^2(E_B)}, \tag{29}$$

where

$$\begin{aligned}\frac{1}{\tau_0(E_B)} &\equiv \frac{1}{\tau_+(\mu,E_B))}\equiv\frac{1}{\tau_-(\mu,E_B))}\\ &= 1.5\,\omega_0(E_B)\exp\left(-\frac{E_B-\mu}{k_BT}\right).\end{aligned} \tag{30}$$

Our actual system is characterized only by the weaker inequalities $z_T < r_s$, $2k_BT < \Delta E_B$. Therefore, for comparison with experiments we shall still use the original formula (27). At the same time, for the qualitative analysis, we will focus on Eq.(29), but all the conclusions will be fully applicable to Eq.(27).

A remarkable feature of Eq.(29), which can be traced back to Eq.(7), is that, even though the resistance noise is caused by the fluctuations in the number of conduction electrons, the resulting noise spectrum is independent of their equilibrium concentration. Furthermore, that spectrum is only weakly dependent on all the defect parameters involved (see Ref.[18]). In particular, the dependence of the prefactor on the concentration of defects n_D is balanced by the $n_D^{-1/2}$ dependence of r_{s2}, which then enters r_s^3 via Eq.(23).

Like in the BDAE model, the $1/f$-like spectral shape generated by formula (29) is the result of the broad distribution of the activation energies $P(E_B)$, but, at the same time, formula (29) has also two new features, namely: (i) the $1/T$ dependence of the prefactor and (ii) the energy-dependent weight $r_s^3\left(\tau(E_B)\right)$ multiplying $P(E_B)$. The second feature is particularly important for extracting the correct distribution of $P(E_B)$ from experimental data.

For comparison with experiment in Section VII we will need the integral of $\frac{S_V(f)}{V^2}$ over all frequencies, which is equal to $C_V(0)$. The expression for $C_V(0)$ can be obtained by substituting $\frac{1}{4}r_s^4(\tau)\Big[4z_T-3r_s(\tau)+e^{-\frac{2z_T}{r_s(\tau)}}(2z_T+3r_s(\tau))\Big]$ instead of $D(f,\tau)$ into Eq.(27). The mathematical structure of this expression is similar to Eq.(27) but otherwise not very illuminating to be written explicitly one more time. Instead, we give an estimate for the noise integral corresponding to the thin film limit (29). We do it with one further simplification. Namely, we replace $r_s(\tau(E_B))$ in Eq.(29) by the typical value $r_s^*=0.2\ \mu$m and then obtain:

$$\int_0^\infty\frac{S_V(f)}{V^2}\,df=\frac{2\pi^2e^4n_Dr_s^{*3}}{\epsilon^2k_BT\ \Delta E\ A}. \tag{31}$$

Although the bulk limit $z_T \gg r_s$ appears to be incompatible with the assumption of independent defect fluctuations (to be explained in Section VIII), it is still instructive to give an expression for the noise integral in this case too. Combining the limit $z_T \gg r_s$ with all other approximations used to derive Eq.(31), we obtain

$$\int_0^\infty\frac{S_V(f)}{V^2}\,df=\frac{4\pi^2e^4n_Dr_s^{*4}}{\epsilon^2k_BT\ \Delta E\ Az_T}. \tag{32}$$

Up to numerical prefactors, both approximations (31) and (32) can be summarized as follows: the noise intensity is proportional to $\left(\frac{e}{k_BT}\right)^2$, multiplied by the mean squared amplitude of potential fluctuations $\frac{e^2n_Dk_BTr_s^*}{\epsilon^2\Delta E}$, further multiplied by the screening volume of a typical fluctuation r_s^{*3}, and, finally, divided by the volume of the space, where the defects contributing to the potential fluctuations are located. In the thin layer limit that volume is roughly $2r_sA$, whereas in the bulk limit it is $2z_TA$. The combination $n_Dk_BT/\Delta E$ appearing in the estimate of the potential fluctuation should be identified with the concentration of "thermally active" defects, i.e. those defects that fall in the thermal energy window around the chemical potential.

Now we give various estimates of the prefactor in front of the approximate $1/f$ dependence of the spectrum. For the thin film limit, we start from Eq.(29) and

then, assuming $r_s(\tau(E_B)) = r_s^*$, $P(E_B) = \frac{1}{2\Delta E_B}$ and $\omega_0(E_B) = \omega_0(E_{B0})$, obtain

$$\frac{S_V(f)}{V^2} = \frac{\pi^2 e^4 n_D r_s^{*3}}{\epsilon^2 A\ \Delta E\ \Delta E_B}\ \frac{1}{f}. \tag{33}$$

For the bulk limit, the analogous expression is

$$\frac{S_V(f)}{V^2} = \frac{2\pi^2 e^4 n_D r_s^{*4}}{\epsilon^2 A z_T\ \Delta E\ \Delta E_B}\ \frac{1}{f}. \tag{34}$$

Equation(34) admits yet another remarkable simplification, if one substitutes $r_{\rm eq}$ given by Eq.(17) instead of r_s^*. (The equilibrium self-screening mechanism described by Eq.(17) should indeed be a proper description for the slower fraction of the defects, which means the lower frequency part of the spectrum.) In this case

$$\frac{S_V(f)}{V^2} = \frac{\Delta E}{2Az_T n_D \Delta E_B}\ \frac{1}{f} \sim \frac{1}{N_D f}, \tag{35}$$

where $N_D = 2Az_T n_D$ is the total number of defects in the constant resistivity layer. [In the above approximation, we assumed $\Delta E \sim \Delta E_B$.] Although this result looks like a standard statistical factor, its origin is, in fact, far more complex. It can be traced back to an accidental interplay between the resistivity fluctuations and the screening mechanism. Given the limitations of the "bulk limit", it is unlikely that formula (35) represents a clean limit in any realistic system. At the same time, for $r_s \sim z_T$, this formula still gives a reasonable estimate.

It is, finally, interesting to observe that, for the numbers characterizing our system, the Hooge's formula[23] $\frac{S_V(f)}{V^2} = \frac{\alpha}{N_C f}$ with coefficient $\alpha \sim 10^{-3}$, would produce an estimate close to that of Eq.(35), (Here N_C is the total number of conduction electrons.) This simply reflects the fact, that in our case the concentration of conduction electrons is about thousand times smaller than the concentration of defects. The exact ratio of these concentrations is strongly temperature dependent, as is the value of α required to fit the noise intensity in our experiments.

VII. COMPARISON WITH EXPERIMENT

Theoretical spectra computed from Eq.(27) are compared with the experimental ones in Fig. 2a (see also Ref.[24]). The experimental spectra were obtained by subtracting the zero-current noise from the total noise observed with $V = 50$ meV. They were consistent with the spectra reported in Ref.[10], though the film was newly grown. All the theoretical spectra were obtained with $P(E_B)$ shown in Fig. 2b and characterized by $E_{B0} = \mu + 0.90\,\text{eV}$ and $\Delta E_B = 0.09\,\text{eV}$. The uncertainties of the fit for E_{B0} and ΔE_B are 0.05 eV and 0.02 eV, respectively. Figure 2c shows $r_s(E_B)$ obtained by averaging $r_s\left(\tau_+(E, E_B)\right)$ and $r_s\left(\tau_-(E', E_B)\right)$ over E and E' at $T = 434\,\text{K}$. Finally, Fig. 2d illustrates the role of the

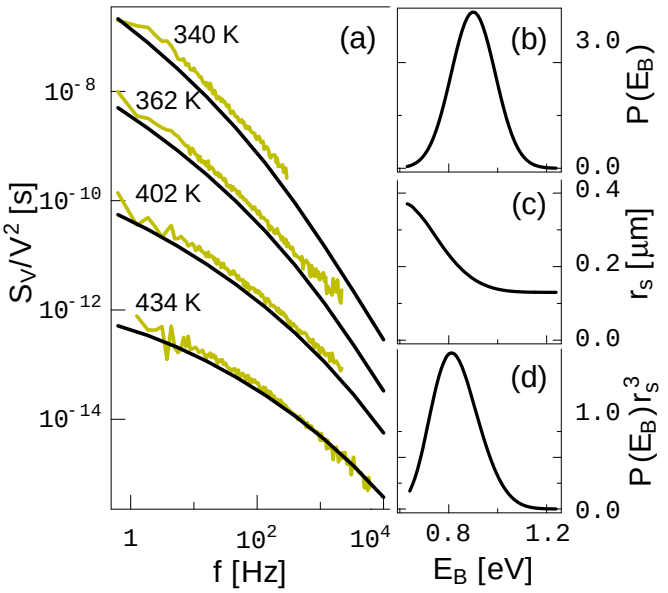

FIG. 2: (a) Noise spectra: erratic lines — experiment, smooth lines — predictions of Eq.(27). The spectra at 340K, 362K and 402K are multiplied, respectively, by 30^3, 30^2 and 30 to make them distinguishable. On the real scale all four spectra fall almost on the top of each other. (b-d) Probability distribution $P(E_B)$, the screening radius r_s and the product $P(E_B)r_s^3$ as functions of the barrier energy E_B counted from $\mu = 0$.

r_s^3 weight by showing $P(E_B)r_s^3(E_B)$. If $P(E_B)$ were to be obtained by fitting the experimental spectra to the BDAE model[10], the result would look like Fig. 2d, i.e. the maximum would be shifted by about 0.1 eV in comparison with Fig. 2b.

With the above value of ΔE_B, the estimates (33,34,35) for the prefactor in front of $1/f$ would give respectively: $9 \cdot 10^{-12}$, $3 \cdot 10^{-11}$ and $1 \cdot 10^{-11}$ — all in reasonable agreement with experiments. [For the estimates (34) and (35) we used $z_T = 0.13$ μm.]

In Fig. 3 we present another test of our theory, which is independent of the choice of E_{B0} and ΔE_B. Namely, we compare the theoretical and experimental values of the integrated noise intensities for the four temperatures indicated in Fig. 2a.

The experimental evaluation of the integrated intensity of an $1/f$-like noise is a task notorious for its ambiguity. Fortunately, in our case, the power law extrapolations of all four noise spectra were convergent, which allowed us to use the following procedure:

First, we obtained the lower ends of the error bars by integrating the experimental noise spectra only in the frequency range of the actual experimental observations. Then, the upper ends were obtained by making power law extrapolations of the spectra beyond the frequency range of observation (up to 10^{-6} Hz for small frequencies and 10^8 Hz for large frequencies), and then adding the integrals over the extrapolated tails to the lower end values of the error bars. Finally, the "experimental" points indicated in Fig. 3 were chosen as the middle points of

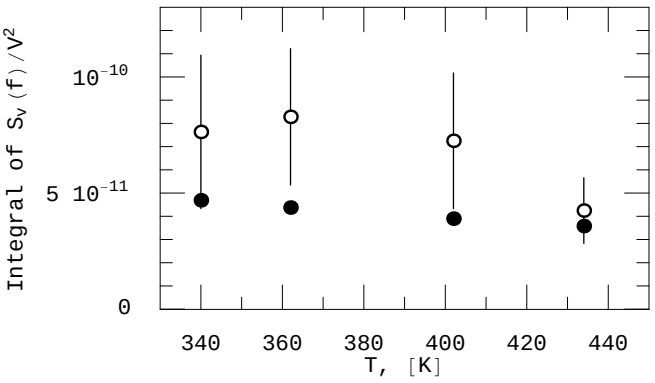

FIG. 3: Integrated noise intensity for the four spectra presented in Fig. 2. Empty dots represent experimental values, and the solid black dots theoretical values obtained from Eq.(27). The error bars on the experimental points are obtained as described in the text

the above error bars.

The theoretical points presented in Fig. 3 were obtained for the full spectrum (27) as described in Section VI. One can also check that the estimate (31) gives numbers, which are not much different, e.g.: $5.6 \cdot 10^{-11}$ for $T = 340$ K, and $4.4 \cdot 10^{-11}$ for $T = 434$ K.

Given the large uncertainties of the extrapolation and the theoretical uncertainties indicated earlier, the factor of two agreement between the theoretical and experimental points in Fig. 3 should be considered as a successful consistency test of the noise mechanism proposed.

VIII. POSSIBLE GENERALIZATIONS

Now we discuss briefly various modifications required in order to generalize our treatment to $1/f$ noise experiments in other settings involving a-Si:H.

The application of the present theory to the films with coplanar currents[9,11,12,14,15] and also to the bulk samples would encounter an essential complication related to the absence of contact layers. In this case, the charge fluctuations of different defects become correlated via emission and capture of the same electron. In such a process, the potential fluctuation is simply translated in space from one defect to another, which means that, unless the two defects have different screening radii, the total resistance does not fluctuate at all. Our analysis in Section V revealed one possibility for different defects to have different screening radii (as a function of their activation times). However, even with this possibility, the overall effect of the absence of contact layers should be a noticeable reduction of the noise intensity.

The contact layers also play a role in the screening of defects. Without them (and without the n-layers) the first screening mechanism considered in Section V is not operational. Therefore, the treatment of screening of the faster fluctuating defects becomes more difficult.

The theory has to be further modified to include the hole conduction, if, as a result of doping, the chemical potential moves in the middle or below the middle of the band gap. An interesting situation may arise, when hole resistivity is equal to electron resistivity. In this case one should expect a drastic reduction of the noise intensity, because the change of electron resistivity induced by potential fluctuations will be compensated by the change in the hole resistivity.

Analysing experiments, one should also keep in mind that creation and annealing of charged defects represents an alternative way to potential fluctuations. In particular, in a-Si:H such a process may be associated with the diffusion of hydrogen atoms[16], which can inhibit or expose the dangling bonds. The parameters describing this process are not very well known. In our case, the mechanism involving the emission and the capture of conduction electrons by already existing defects appears to be sufficient, but, in general, creation and annealing of defects can lead to a comparable contribution to the integrated noise intensity.

Summarizing this Section, we would like to emphasise that all the above complications can still be treated on the basis of formula (7), but different ingredients for the evaluation of the potential fluctuations will be required.

IX. CONCLUSIONS

In conclusion, we have developed a microscopic theory of $1/f$ noise in $n-i-n$ sandwich structures of a-Si:H and found a very good agreement between this theory and our experiments. The noise mechanism proposed should be quite general (in particular, in semiconductors): it merely requires the presence of charge traps in regions of poor screening. The full calculation of the actual noise spectrum necessarily involves a fair amount of material specific details, which, to some extent, mask the generality of our treatment. However, one should remember, that our calculation is based on formula (7), which appears to have quite a broad range of applicability.

From a different perspective, our analysis introduces a new method of characterizing the deep defects in a-Si:H. In particular, our finding, that $E_{B0} - E_{c0} = 0.27\,\mathrm{eV}$, which is substantially greater than 0.1 eV — the scale of potential fluctuations seen in the drift mobility experiments[16], may indicate that the defects are not distributed randomly in the background of the medium-range random potential but, instead, located in the regions of greater local strain, i.e. around the peaks of that potential.

Our result also limits the spectral intensities due to all other possible noise mechanisms to the difference between the experimental spectra and the spectra given by Eq.(27). Even with the freedom of varying E_{B0} and ΔE_B, this is a very strong constraint.

Acknowledgments

We thank R. E. I. Schropp for providing us with the sample, and A. Buchleitner, B. Farid and M. Weissman for their helpful comments on the manuscript. The work of B. V. F. was supported by the Foundation of Fundamental Research on Matter (FOM), which is sponsored by the Netherlands Organization for the Advancement of Pure Research (NWO).

* E.mail: fine@mpipks-dresden.mpg.de

[1] J. B. Johnson, Phys. Rev. **32**, 97 (1928);
[2] H. Nyquist, Phys. Rev. **32**, 110 (1928)
[3] M. B. Weissman, Rev. Mod. Phys. **60**, 537 (1988).
[4] A. van der Ziel, Physica (Utrecht) **16**, 359 (1950).
[5] F. K. du Pre, Phys. Rev. **78**, 615 (1950).
[6] P. Dutta, P.Dimon and P.M.Horn, Phys. Rev. Lett. **43**, 646 (1979).
[7] F. Z. Bathaei and J. C. Anderson, Philos. Mag. B **55**, 87 (1987).
[8] M.Baciocchi, A.D'Amico and C.M.van Vliet, Solid-St. Electron. **34**, 1439 (1991).
[9] G. M. Khera and J. Kakalios, Phys. Rev. B **56**, 1918 (1997).
[10] P. A. W. E. Verleg and J. I. Dijkhuis, Phys. Rev. B **58**, 3904 (1998).
[11] M. Günes, R.E. Johanson, and S.O. Kasap, Phys. Rev. B. 60, 1477 (1999).
[12] R. E. Johanson *et al.*, J. Vac. Sci. Technol. A **18(2)**, 661 (2000).
[13] S. T. B. Goennenwein *et al.*, Phys. Rev. Lett. **84**, 5188 (2000).
[14] T. J. Belich and J. Kakalios, Phys. Rev. B **66**, 195212 (2002).
[15] S. O. Kasap *et al.*, J. Mater. Sci.: Materials in Electronics, in press, October 2003 issue.
[16] R. A. Street, *Hydrogenated amorphous silicon* (Cambridge University Press, Cambridge, 1991).
[17] J. P. R. Bakker, B. J. van der Horst and J. I. Dijkhuis, J. Non-Cryst. Solids **299-302**, 1256 (2002).
[18] In what follows, the values of n_D, E_0 and ΔE were obtained from numerical fit to the non-linear IV-characteristics of our film taken at high applied voltages (cf.[17]). The values of U, m_e^*, σ, $N_c(E_{c0})$ and ε_c represent the most general practice (see e.g.[16]).
[19] M. Stutzmann, W. B. Jackson, and C. C. Tsai, Phys. Rev. B. **32**, 23 (1985).
[20] D. Adler and E. Yoffa, Phys. Rev. Lett. **36**, 1197 (1976).
[21] A. D. van Rheenen, G. Bosman and R. J. J. Zijlstra, Solid-St. Electron. **30**, 259 (1987).
[22] B.I.Shklovskii, A.L.Efros, *Electronic Properties of Doped Semiconductors* (Springer-Verlag, Berlin, 1984), Ch.3.3.
[23] F. N. Hooge, Phys. Lett. A **29**, 139 (1969).
[24] See EPAPS Document No. ... for the figures illustrating weak sensitivity of the theoretical spectra shown in Fig. 2(a) to the variations of n_D, ΔE, E_0 and U.